machines

MDPI

Article

Prescribed Performance Trajectory Tracking Control for Electro-Hydraulic Servo Pump-Controlled Systems with Input and State Delays

Gengting Qiu [1], Yujie Hao [1], Gexin Chen [1,2,*], Guishan Yan [2,3] and Yao Chen [4]

[1] School of Mechanical Engineering, Yanshan University, Qinhuangdao 066000, China; gengtingqiu@163.com (G.Q.); haoyujie0364@163.com (Y.H.)
[2] Xinjiang Coal Mine Electromechanical Engineering Technology Research Center, Xinjiang Institute of Engineering, Urumqi 830023, China; ygs@xjie.edu.cn
[3] National Key Laboratory of Metal Forming Technology and Heavy Equipment, China National Heavy Machinery Research Institute Co., Ltd., Xi'an 710018, China
[4] Shougang Jingtang United Iron & Steel Co., Ltd., Tangshan 063000, China; 15832555802@163.com
* Correspondence: cgx@xjie.edu.cn

Abstract

Electro-hydraulic servo pump-controlled systems have advantages such as energy saving and high integration and are widely applied in aerospace, engineering machinery, and other fields. However, the input and state delays introduced by drive circuit, control period, and oil leakage result in lower dynamic response speed compared to traditional valve control systems, which restricts the promotion of the system. In this paper, a prescribed performance trajectory tracking control method is proposed to improve the transient and steady-state performance of the system. A performance function is designed to constrain the range of trajectory tracking errors. The constrained space is mapped to an unconstrained space via a homeomorphic transformation, and the control laws are designed by integrating it with the backstepping method. In the final step of the backstepping design, the input and state delays are processed using Lyapunov–Krasovskii functionals. The simulation and experimental results show that under the condition of fixed input delay and state delay, the trajectory tracking errors converge within the preset range, and all states of the system are uniformly bounded. The results demonstrate the effectiveness of the proposed method in this paper.

Keywords: electro-hydraulic servo pump-controlled systems; prescribed performance control; trajectory tracking; input and state delays

check for updates

Academic Editor: Piotr Czop

Received: 12 November 2025
Revised: 1 December 2025
Accepted: 12 December 2025
Published: 17 December 2025

Citation: Qiu, G.; Hao, Y.; Chen, G.; Yan, G.; Chen, Y. Prescribed Performance Trajectory Tracking Control for Electro-Hydraulic Servo Pump-Controlled Systems with Input and State Delays. *Machines* **2025**, *13*, 1147. https://doi.org/10.3390/machines13121147

Copyright: © 2025 by the authors. Licensee MDPI, Basel, Switzerland. This article is an open access article distributed under the terms and conditions of the Creative Commons Attribution (CC BY) license (https://creativecommons.org/licenses/by/4.0/).

1. Introduction

Electro-hydraulic servo pump-controlled systems are widely used in high-power density drive fields such as industrial machine tools [1–3], engineering vehicles [4,5], aerospace [6], and robotics [7,8], and are the core component of power transmission and control. Compared with valve-controlled hydraulic systems, pump-controlled hydraulic systems have the advantages of low noise, compact structure, high energy conversion efficiency, and reliability [9–11]. In line with the themes of energy conservation and green manufacturing, pump-controlled systems have received increasing attention and become a current research hotspot [12]. However, there exists an input delay phenomenon in electro-hydraulic servo pump-controlled systems which is caused by the sensor signal's transmission delay, the controller's operation period, the servo driver's filtering algorithm,

the current loop response speed in the electrical part, the moment of inertia and connection stiffness of the motor-pump unit in the mechanical part, and oil leakage in the hydraulic part [13,14]. Meanwhile, different from the pre-pressurization of valve control systems, the pressure build-up rate in pump-controlled systems is determined by the compression cavity volume, the oil's bulk modulus, and the load, which leads to state delays in the process of pressure establishment [15,16]. The existence of input and state delays significantly degrades the performance of the pump-controlled system, causing oscillations, increased overshoot, slow responses, and even instability [17]. These issues become the main obstacle to achieving high-precision control and rapid responses in pump-controlled hydraulic systems. Therefore, it is necessary to propose reasonable control methods to improve the system's control performance degradation caused by time-delay phenomena and enhance the system's transient and steady-state performance.

The inherently strong coupling among the electrical, mechanical, and hydraulic subsystems in electro-hydraulic servo pump-controlled systems introduces significant nonlinear behavior. These nonlinearities mainly include dead zones, time delays, and friction, which seriously impair the control accuracy and response speed of the system. To address these issues, relevant scholars have conducted extensive research on nonlinear control strategies to suppress nonlinear disturbances and improve system stability. The traditional PID controller has limited adjustable parameters and often fails to achieve satisfactory control performance due to the inherent nonlinearities and unavoidable uncertainties in hydraulic systems. To solve this problem, an intelligent PID controller is designed for the position control of a nonlinear electro-hydraulic system with uncertain valve characteristics and supply pressure variations in [18], the results show that the controller achieves better tracking results against system uncertainties and external disturbances. In [19], an adaptive robust motion control strategy is proposed to resolve the issue of nonlinear pump flow at low speeds for a direct-driven electro-hydraulic system with adaptive pump flow rate model compensation. A robust high-precision position control strategy incorporating leakage and friction compensation is designed for electro-hydrostatic actuators in [20]; both the steady-state and transient position tracking performances achieve significant improvement. In [21], an adaptive neural network control is designed to compensate for unknown system dynamics based on the backstepping control framework. Additionally, extended state observers are employed to address the disturbance and unknown dynamics. To improve the working performance of electro-hydrostatic actuators, a sliding-mode control strategy with a damping variable sliding surface is proposed in [22]. The simulation and experimental results show that the controller exhibits strong overshoot suppression and robustness. Reference [23] combines a modified backstepping algorithm with a special adaptation law to compensate for all nonlinearities and uncertainties in pump-controlled electrohydraulic actuators. In [24], a position controller is built based on the quantitative feedback theory to satisfy the tracking, stability, and disturbance rejection specifications of electro-hydrostatic actuators. The results show great control performance over a wide range of parametric uncertainties. The above control methods effectively address the issue of control performance degradation in hydraulic systems caused by nonlinearity and uncertainty. However, robust control is inherently conservative, sliding-mode control suffers from chattering, and neural network control demands substantial real-time computation for online learning. More importantly, the design of these controllers fails to account for the effects of input and state delays.

Some control methods have been proposed to compensate for input and state delays such as the Smith predictor [25] and the finite spectrum assignment method [26]. However, these methods suffer from weak robustness and require high model accuracy. In recent years, several control schemes have been developed to enhance the control performance

of nonlinear systems with input and state delays. A controller combining backstepping design and finite-time command filtering technology is proposed in [27]; the results show the convergence of tracking errors and the boundedness of all closed-loop signals for nonlinear systems with input delays. An adaptive neural network controller is presented in [28] to address the trajectory tracking problem for a class of strict-feedback nonlinear systems with state constraints and input delays. Although the aforementioned methods have achieved certain results in dealing with the time-delay phenomena, they fail to restrict the overshoot and convergence speed in the motion process. For switched nonlinear MIMO time-delay systems, an output–feedback method based on funnel control is proposed in [29], ensuring that the tracking error remains within a pre-specified performance funnel. Prescribed performance control (PPC) is first proposed in [30] to constrain the tracking error within a pre-defined bound with exponentially converging performance boundaries, which can achieve specific system performance requirements such as maximum overshoot, convergence rate, and steady-state error [31–34]. However, it is a significant challenge to directly apply PPC to electro-hydraulic servo pump control systems with input and state delays. This is primarily because the presence of delays tends to undermine the stability of error transformation. The Lyapunov–Krasovskii functional method and the Lyapunov–Razumikhin functional method can effectively handle input and state delays in nonlinear systems [35,36]. However, the computational complexity, conservatism, and the need for accurate mathematical models have hindered the widespread application of these functional methods in electro-hydraulic servo pump-controlled systems.

Inspired by the above discussion, combining PPC with the Lyapunov–Krasovskii method is a worthwhile exploration to address the position tracking problem of electro-hydraulic servo pump control systems with input and state delays. The main contributions of this paper are summarized as follows.

(1) The PPC method is introduced into the trajectory tracking of electro-hydraulic servo pump-controlled systems. A performance function is employed to precisely regulate the transient parameters (such as overshoot and convergence speed) of trajectory tracking errors. Through error transformation, the complex nonlinear control problem with state constraints is converted into a standard unconstrained nonlinear stabilization problem, simplifying the processes of controller design and stability analysis.
(2) A state transformation is designed to convert the system with time delays into a time-delay-free equivalent system. The combination of the backstepping control framework and PPC enhances the system's robustness under input and state delay conditions.
(3) Through comparative experiments with traditional PID and backstepping control, the superiority and practical value of the proposed method in real systems have been verified.

The remainder of this paper is organized as follows. Section 2 presents the mathematical model and problem formulation of the electro-hydraulic servo pump-controlled systems with input and state delays. The detailed design procedure of the prescribed performance trajectory tracking controller is elaborated in Section 3. Section 4 provides a rigorous stability analysis. The experimental results of Section 5 verify the effectiveness of the proposed method. Finally, Section 6 concludes the paper.

2. Problem Statement

The working principle of electro-hydraulic servo pump-controlled systems involves controlling the flow rate and pressure supplied to the actuator by adjusting either the speed of the servo motor or the displacement of the hydraulic pump. Based on different control methods, electro-hydraulic servo pump-controlled systems can be divided into three types:

fixed speed and variable displacement, variable speed and variable displacement, and variable speed and fixed displacement. Among these, although the first two types exhibit excellent transient and steady-state performance, they suffer from several drawbacks, including strict requirements for oil cleanliness, the complexity of variable-displacement mechanisms, and throttling or overflow losses. These issues not only reduce the system's reliability and lower energy utilization efficiency but also limit its applicability in certain scenarios. By contrast, the variable speed and fixed displacement control mode has the advantages of a straightforward working principle, high energy efficiency, and low noise. Therefore, it serves as the primary research focus of this paper. Its working principle is illustrated in Figure 1.

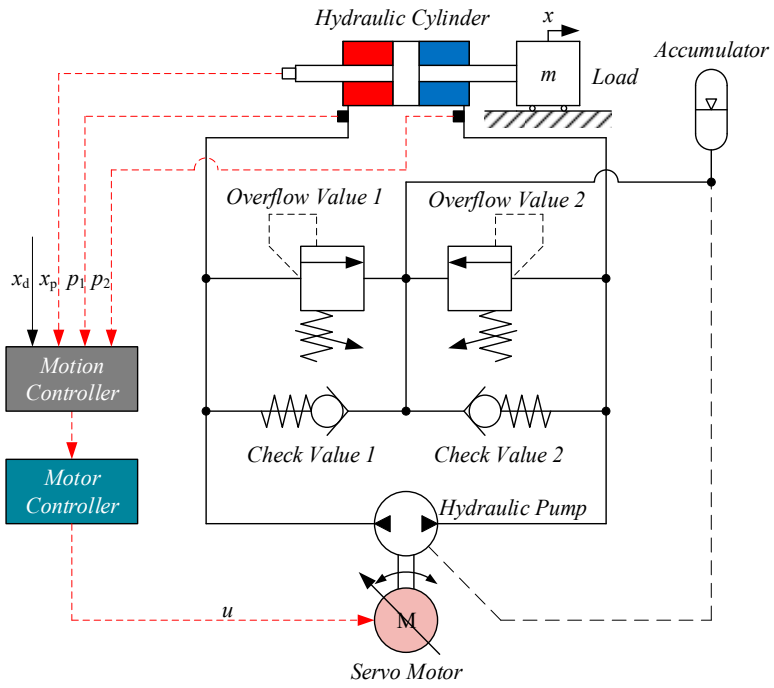


Figure 1. The operating principle of electro-hydraulic servo pump-controlled systems.

As shown in Figure 1, the motor controller drives the servo motor to run a bidirectional fixed displacement hydraulic pump. By adjusting the speed of the servo motor, the flow rate and direction of hydraulic oil are regulated so that the oil enters the two chambers of the cylinder, which pushes the piston to move the load. A small auxiliary accumulator and the check valves are designed to maintain a low pressure in the system's return lines and supplement internal leaks, which can prevent cavitation and ensure stable system operation. The function of the overflow valves is to prevent core components from bursting, sealing damage, or structural deformation due to overpressure. The feedback signals x_p, p_1, p_2 from displacement or pressure sensors are compared with the command signal x_d in the motion controller. Then, the motion controller calculates the system input signal based on the tracking error and subsequently sends it to the motor controller. The motor controller converts the control signal into a high-voltage power signal capable of driving the motor and achieves precise regulation of motor speed.

The fixed displacement pump, serving as the hydraulic power source of the electro-hydraulic servo pump control system, supplies the system with pressure and flow. The flow continuity equation for the fixed displacement pump is formulated as follows.

$$Q_p = D_p N_p - C_{tp} p_L \tag{1}$$

Among these parameters, Q_p denotes the pump output flow, D_p is the displacement of the fixed displacement pump, N_p represents the motor speed, C_{tp} stands for the total leakage coefficient accounting for both internal and external leakage, p_L refers to the load pressure defined as $p_L = p_1 - p_2$, and p_1, p_2 are the pressures in the two chambers of the hydraulic cylinder.

The hydraulic cylinder, serving as an actuator, regulates the displacement and velocity of the load, and its flow continuity equation is as follows.

$$Q_L = A_p \dot{x}_p + C_{tc} p_L + \frac{V_t}{4\beta_e} \dot{p}_L \tag{2}$$

Among these parameters, Q_L denotes the load-required flow, A_p is the effective working area of the hydraulic cylinder, x_p is the piston displacement, and C_{tc} represents the cylinder's leakage coefficient. V_t stands for the hydraulic cylinder's effective volume and β_e refers to the oil's bulk modulus of elasticity.

Considering only the inertia load, the load force balance equation of the hydraulic cylinder can be written as follows.

$$A_p p_L = m_t \ddot{x}_p \tag{3}$$

where m_t is the mass of load. Neglecting the overall effect of the interconnecting volume between the hydraulic pump and hydraulic cylinder, we have $Q_p = Q_L$. Assuming C_{tp}, C_{tc}, β_e are constants, and defining state variable $x = [x_1, x_2, x_3]^T = \left[x_p, \dot{x}_p, A_p p_L / m_t\right]^T$, then the state space equation of the electro-hydraulic servo pump-controlled system is established as follows.

$$\begin{cases} \dot{x}_1 = x_2 \\ \dot{x}_2 = x_3 \\ \dot{x}_3 = \theta_1 u + \theta_2 x_2 + \theta_3 x_3 \end{cases} \tag{4}$$

where $\theta_1, \theta_2, \theta_3$ are known nonlinear functions and can be defined as follows.

$$\theta = [\theta_1, \theta_2, \theta_3]^T = \left[\frac{4A_p \beta_e D_p}{m_t V_t}, -\frac{4A_p^2 \beta_e}{m_t V_t}, -\frac{4\beta_e C_t}{V_t}\right]^T \tag{5}$$

The above equation captures the dynamic characteristics of the electro-hydraulic servo pump-controlled system. However, it ignores the negative impact caused by time delays. Several factors in the electrical control process contribute to system input delay, including sensor signal transmission, the computational load of the control algorithm, the response speed of the motor controller, and the motor's moment of inertia. Meanwhile, during the hydraulic transmission process, the state delays are mainly caused by the coupling effect between the hydraulic chamber and the load. On one hand, an excessively large hydraulic chamber volume reduces system stiffness and prolongs the pressure build-up process; on the other hand, the dynamic characteristics of the load directly influence the pressure build-up process. These two factors collectively result in significant state delays. Therefore, considering the input and state delays of the electro-hydraulic servo pump-controlled system, the state space equation can be modified as follows.

$$\begin{cases} \dot{x}_1(t) = x_2(t) \\ \dot{x}_2(t) = x_3(t) \\ \dot{x}_3(t) = \theta_1 u(t - \tau_1) + \theta_2 x_2(t) + \theta_2 x_2(t - \tau_2) + \theta_3 x_3(t) + \theta_3 x_3(t - \tau_3) \end{cases} \tag{6}$$

where τ_1, τ_2, τ_3 are known time-delay constants.

Assumption 1. *The system states satisfy* $|x_i(t)| \leq X_i, \forall t \in [0, \tau], i = 1, 2, 3$, *where* $X_i > 0$ *are positive constants. The target trajectory satisfies* $|x_d(t)| \leq X_d$ *for* $t \in [0, \tau]$.

Remark 1. *The boundedness assumption on the system states and the desired trajectory is not arbitrary but grounded in the physical realities of the electro-hydraulic servo pump-controlled systems. The displacement* $x_1(t)$ *is inherently bounded by the finite stroke length of the hydraulic cylinder. The velocity* $x_2(t)$ *is bounded by the maximum flow rate deliverable by the fixed-displacement pump, which is determined by the pump's displacement and the servo motor's maximum speed. The state* $x_3(t)$ *is bounded by the preset cracking pressure of the system's relief valves, which serves as a fundamental safety feature. The desired trajectory* $x_d(t)$ *is always designed to be bounded and physically achievable in practice. Therefore, Assumption 1 is not only mathematically convenient but also physically justified and holds for all practical operations of the system.*

Remark 2. *The dynamic model established in this paper focuses on the dominant dynamics and time-delay effects of the system, without explicitly including complex nonlinearities such as friction, changes in the fluid elastic modulus, and pipeline dynamics. We recognize that these unmodeled dynamics can be viewed as bounded uncertainties acting on the system. However, the core advantage of the PPC framework proposed in this paper lies in its inherent robustness to such bounded uncertainties by directly defining the boundaries of tracking errors. The experimental results show that even with these model simplifications, the designed controller can still ensure that the system states are uniformly bounded and the tracking error converges within the preset performance boundary, which fully verifies the effectiveness of the proposed method in practical applications.*

3. Controller Design

PPC predefines the overshoot, convergence rate, and steady-state error of the system through a performance function and incorporates a nonlinear error transformation to ensure that the tracking error remains within the predefined bounds. The backstepping method is suitable for strict-feedback nonlinear systems. Its design follows a "recursive procedure from the outer loop to the inner loop", which means starting from the outermost subsystem to recursively design virtual control variables to stabilize each level subsystem in sequence. Finally, the real control variables are obtained at the innermost layer to achieve global stability of the system. In this section, the backstepping method is adopted as the design framework, and the performance functions and error transformations of PPC are incorporated into the control law design for each subsystem. This enables the achievement of stability and convergence for the displacement, velocity, and pressure states of the electro-hydraulic servo pump-controlled systems with input and state delays. The design steps of the controller are shown below.

To map the normalized error from $(-1, 1)$ onto the entire real axis $(-\infty, +\infty)$, a monotonically increasing nonlinear mapping function $T(\alpha)$ is defined as follows.

$$T(\alpha) = \ln\left(\frac{1+\alpha}{1-\alpha}\right) \tag{7}$$

where $\alpha \in (-1, 1)$ and $lim_{\alpha \to 1^-} T(\alpha) = +\infty$, $lim_{\alpha \to -1^+} T(\alpha) = -\infty$.

Step 1: The performance function $\rho_1(t)$ of the first-order system is proposed as follows:

$$\rho_1(t) = \left(\rho_1^0 - \rho_1^\infty\right) e^{-\lambda_1 t} + \rho_1^\infty \tag{8}$$

where $\rho_1^0 > 0$ is the initial value of the performance function, specifying the maximum allowable overshoot; $\rho_1^\infty > 0$ is its steady-state value, defining the system's maximum

allowable steady-state error; and $\lambda_1 \geq 0$ is its decay rate, setting the minimum convergence rate for the tracking error.

The first-order control law is designed as

$$a_1(x_1, t) = -k_1 T\left(\frac{x_1(t) - x_d(t)}{\rho_1(t)}\right) \tag{9}$$

where $k_1 > 0$ is the control parameter.

Step 2: The performance function $\rho_2(t)$ of the second-order system is proposed as follows:

$$\rho_2(t) = \left(\rho_2^0 - \rho_2^\infty\right)e^{-\lambda_2 t} + \rho_2^\infty \tag{10}$$

where $\rho_2^0 > 0$ is the initial value of the performance function, specifying the maximum allowable overshoot; $\rho_2^\infty > 0$ is its steady-state value, defining the system's maximum allowable steady-state error; and $\lambda_2 \geq 0$ is its decay rate, setting the minimum convergence rate for the tracking error.

The second-order control law is designed as

$$a_2(x_2, t) = -k_2 T\left(\frac{x_2(t) - a_1(t)}{\rho_2(t)}\right) \tag{11}$$

where $k_2 > 0$ is the control parameter.

Step 3: The performance function $\rho_3(t)$ of the third-order system is proposed as follows:

$$\rho_3(t) = \left(\rho_3^0 - \rho_3^\infty\right)e^{-\lambda_3 t} + \rho_3^\infty \tag{12}$$

where $\rho_3^0 > 0$ is the initial value of the performance function, specifying the maximum allowable overshoot; $\rho_3^\infty > 0$ is its steady-state value, defining the system's maximum allowable steady-state error; and $\lambda_3 \geq 0$ is its decay rate, setting the minimum convergence rate for the tracking error.

The third-order control law is designed as follows.

$$u(x_3, t) = -k_3 T\left(\frac{x_3(t) + \theta_1 \int_{t-\tau_1}^{t} u(s)ds + \theta_2 \int_{t-\tau_2}^{t} x_2(s)ds + \theta_3 \int_{t-\tau_3}^{t} x_3(s)ds - a_2(t)}{\rho_3(t)}\right) \tag{13}$$

where $k_3 > 0$ is the control parameter.

To implement the control laws on the motion controller, the discretized form of control law (9) can be expressed as follows.

$$a_1[k] = -k_1 T\left(\frac{x_1[k] - x_d[k]}{(\rho_1^0 - \rho_1^\infty)e^{-\lambda_1[kT_s]} + \rho_1^\infty}\right) \tag{14}$$

where $T_s = 1$ ms is the sampling period of the motion controller and k is the index of the discrete time series.

The discretized form of control law (11) can be expressed as follows.

$$a_2[k] = -k_2 T\left(\frac{x_2[k] - a_1[k]}{(\rho_2^0 - \rho_2^\infty)e^{-\lambda_2[kT_s]} + \rho_2^\infty}\right) \tag{15}$$

The discretized form of control law (13) can be expressed as follows.

$$u[k] = -k_3 T\left(\frac{x_3[k] + \theta_1 T_s \sum_{i=k-N_1}^{k} u[i] + \theta_2 T_s \sum_{i=k-N_2}^{k} x_2[i] + \theta_3 T_s \sum_{i=k-N_3}^{k} x_3[i] - a_2[k]}{(\rho_3^0 - \rho_3^\infty)e^{-\lambda_3[kT_s]} + \rho_3^\infty}\right) \tag{16}$$

where $N_i = \tau_i / T_s$ and τ_i are integer multiples of T_s with $i = 1, 2, 3$.

To define the behavior of the controller when $t \in [-\tau, 0)$, set the historical initial value of the controller as $u(t) = x_2(t) = x_3(t) = 0$ for all $t \in [-\tau, 0)$. Then,

$$\int_{-\tau_1}^{0} u(s)ds = \beta_1,\ \int_{-\tau_2}^{0} x_2(s)ds = \beta_2,\ \int_{-\tau_3}^{0} x_3(s)ds = \beta_3 \tag{17}$$

where $\beta_1, \beta_2, \beta_3$ are constants.

4. Stability Analysis

The coordinate transformation for the state variables of the electro-hydraulic servo pump-controlled system is as follows.

$$\begin{cases} z_1 = x_1 \\ z_2 = x_2 \\ z_3 = x_3 + \theta_1 \int_{t-\tau_1}^{t} u(s)ds + \theta_2 \int_{t-\tau_2}^{t} x_2(s)ds + \theta_3 \int_{t-\tau_3}^{t} x_3(s)ds \end{cases} \tag{18}$$

Then, the state-space representation (6) can be transformed as follows.

$$\begin{cases} \dot{z}_1 = z_2 \\ \dot{z}_2 = z_3 - \theta_1 \int_{t-\tau_1}^{t} u(s)ds - \theta_2 \int_{t-\tau_2}^{t} x_2(s)ds - \theta_3 \int_{t-\tau_3}^{t} x_3(s)ds \\ \dot{z}_3 = \theta_1 u(t) + 2\theta_2 z_2 + 2\theta_3 \left(z_3 - \theta_1 \int_{t-\tau_1}^{t} u(s)ds - \theta_2 \int_{t-\tau_2}^{t} x_2(s)ds - \theta_3 \int_{t-\tau_3}^{t} x_3(s)ds \right) \end{cases} \tag{19}$$

The normalized errors are defined as follows.

$$\xi_1 = \frac{z_1 - x_d}{\rho_1}, \xi_2 = \frac{z_2 - a_1}{\rho_2}, \xi_3 = \frac{z_3 - a_2}{\rho_3} \tag{20}$$

By substituting Equations (18) and (20) into (9), (11), and (13), the control laws are transformed as follows.

$$a_1 = -k_1 T(\xi_1), a_2 = -k_2 T(\xi_2), u = -k_3 T(\xi_3) \tag{21}$$

For the subsequent analysis, we define the following transformed errors.

$$\varepsilon_1 = T(\xi_1), \varepsilon_2 = T(\xi_2), \varepsilon_3 = T(\xi_3) \tag{22}$$

Then, the control laws can be transformed as follows.

$$a_1 = -k_1 \varepsilon_1, a_2 = -k_2 \varepsilon_2, u = -k_3 \varepsilon_3 \tag{23}$$

Further, the derivative of normalized errors can be expressed as follows.

$$\begin{aligned} \dot{\xi}_1 &= \frac{1}{\rho_1} \left[\xi_2 \rho_2 - \dot{x}_d - \xi_1 \dot{\rho}_1 - k_1 T(\xi_1) \right] \\ \dot{\xi}_2 &= \frac{1}{\rho_2} \left[\xi_3 \rho_3 - \dot{a}_1 - \xi_2 \dot{\rho}_2 - \theta_1 \int_{t-\tau_1}^{t} u(s)ds - \theta_2 \int_{t-\tau_2}^{t} x_2(s)ds - \theta_3 \int_{t-\tau_3}^{t} x_3(s)ds - k_2 T(\xi_2) \right] \\ \dot{\xi}_3 &= \frac{1}{\rho_3} \left[\begin{array}{l} 2\alpha_3 \left(\xi_3 \rho_3 + a_2 - \theta_1 \int_{t-\tau_1}^{t} u(s)ds - \theta_2 \int_{t-\tau_2}^{t} x_2(s)ds - \theta_3 \int_{t-\tau_3}^{t} x_3(s)ds \right) \\ +2\alpha_2 (\xi_2 \rho_2 + a_1) - \dot{a}_2 - \xi_3 \dot{\rho}_3 - \theta_1 k_3 T(\xi_3) \end{array} \right] \end{aligned} \tag{24}$$

Define an open set $\Omega_\xi = (-1, 1)^3 \subset \mathbb{R}^3$, and when the normalized errors ξ, in Equation (20) satisfy $\xi \in \Omega_\xi$, the tracking error of the system achieves the predetermined performance requirements. However, it is difficult to directly prove $\xi \in \Omega_\xi$, so the nonlinear mapping function $T(\alpha)$ is introduced to convert the error region to $(-\infty, +\infty)$. Based on

the properties of the $T(\alpha)$, when the transformed errors ε, are bounded, the normalization errors ξ, are included in $\Omega_{\bar{\xi}}$, and the stability of the system can be proven. From Assumption 1, we have $\xi \in \Omega_{\bar{\xi}}$ for $t \in [0, \tau]$. According to the existence and uniqueness theorem for ordinary differential equation solutions, there exists a finite escape time $\tau_f \in (0, \infty]$ such that $\xi \in \Omega_{\bar{\xi}}$ for all $t \in \left[0, \tau_f\right)$.

Based on the above discussion, we now utilize the backstepping framework to prove the boundedness of all signals in the closed-loop system after error transformation, thereby establishing that the tracking error converges with prescribed performance.

Step 1: The Lyapunov function constructed for the first-order system is as follows:

$$V_1 = \frac{1}{2}\varepsilon_1^2 \tag{25}$$

By substituting Equations (12), (13), and (18) into the differential of Equation (25), we can obtain

$$\dot{V}_1 = \frac{2\varepsilon_1}{(1-\xi_1^2)\rho_1}\left(\xi_2\rho_2 - \dot{x}_d - \xi_1\dot{\rho}_1 - k_1\varepsilon_1\right) \tag{26}$$

In Equation (26), $\xi_1 \in \Omega_{\bar{\xi}}$ for $t \in \left[0, \tau_f\right)$ can be obtained from the above discussion, and based on the definition of ρ_1, we can obtain $\rho_1 > 0$ for $t \in [0, +\infty)$. Then, it can be concluded that $2/\left((1-\xi_1^2)\rho_1\right) > 0$ for $t \in \left[0, \tau_f\right)$. $\dot{\rho}_1, \rho_2, \dot{x}_d$ are set as bounded. Define $F_1 = |\xi_2\rho_2| + |\dot{x}_d| + |\xi_1\dot{\rho}_1|$ and there exists a positive constant $\overline{F}$, such that $F_1 \leq \overline{F}$ for $t \in \left[0, \tau_f\right)$. Then, $\dot{V}_1$ satisfies the following inequality.

$$\dot{V}_1 \leq \frac{2|\varepsilon_1|}{(1-\xi_1^2)\rho_1}\left(\overline{F}_1 - k_1|\varepsilon_1|\right), \forall t \in \left[0, \tau_f\right) \tag{27}$$

From Equation (27), we can obtain $\dot{V}_1 < 0$ when $|\varepsilon_1| > \overline{F}_1/k_1$; thus,

$$|\varepsilon_1| \leq \bar{\varepsilon}_1 \triangleq \max\left\{|\varepsilon_1(0)|, \frac{\overline{F}_1}{k_1}\right\}, \forall t \in \left[0, \tau_f\right) \tag{28}$$

Combining Equations (22) and (28), the range of conversion tracking errors can be concluded as follows.

$$-1 < T^{-1}(-\bar{\varepsilon}_1) \leq \xi_1 \leq T^{-1}(\bar{\varepsilon}_1) < 1, \forall t \in \left[0, \tau_f\right) \tag{29}$$

By Equations (21) and (29), it can be concluded that the control law a_1 is bounded. From Equations (7), (21), and (29), we can obtain $\left|\dot{a}_1\right| \leq 2k_1\dot{\xi}_1/\left(1-\xi_1^{*2}\right)$, where $\xi_1^* = max\left\{T^{-1}(-\bar{\varepsilon}_1), T^{-1}(\bar{\varepsilon}_1)\right\}$. Hence, $\left|\dot{a}_1\right|$ is bounded for $t \in \left[0, \tau_f\right)$.

Step 2: The Lyapunov function constructed for the second-order system is as follows:

$$V_2 = \frac{1}{2}\varepsilon_2^2 \tag{30}$$

By substituting Equations (12), (13), and (18) into the differential of Equation (30), we can obtain

$$\dot{V}_2 = \frac{2\varepsilon_2}{(1-\xi_2^2)\rho_2}\left(\xi_3\rho_3 - \dot{a}_1 - \xi_2\dot{\rho}_2 - k_2\varepsilon_2 - \theta_1\int_{t-\tau_1}^{t} u(s)ds - \theta_2\int_{t-\tau_2}^{t} x_2(s)ds - \theta_3\int_{t-\tau_3}^{t} x_3(s)ds\right) \tag{31}$$

In Equation (31), $\xi_2 \in \Omega_{\bar{\xi}}$ for $t \in \left[0, \tau_f\right)$ can be obtained from the above discussion, and based on the definition of ρ_2, we can obtain $\rho_2 > 0$ for $t \in [0, +\infty)$. Then, it can be

concluded that $2/\left(\left(1-\xi_2^2\right)\rho_2\right) > 0$ for $t \in \left[0, \tau_f\right)$. $\dot{\rho}_2, \rho_3, \dot{a}_1$ are set as bounded. Define $F_2 = |\xi_3\rho_3| + |\dot{a}_1| + \left|\xi_2\dot{\rho}_2\right| + \left|\theta_1\int_{t-\tau_1}^{t} u(s)s + \theta_2\int_{t-\tau_2}^{t} x_2(s)ds + \theta_3\int_{t-\tau_3}^{t} x_3(s)ds\right|$ and there exists a positive constant $\overline{F}_2$, such that $F_2 \le \overline{F}_2$ for $t \in \left[0, \tau_f\right)$. Then, $\dot{V}_2$ satisfies the following inequality.

$$\dot{V}_2 \le \frac{2|\varepsilon_2|}{\left(1-\xi_2^2\right)\rho_2}\left(\overline{F}_2 - k_2|\varepsilon_2|\right), \forall t \in \left[0, \tau_f\right) \tag{32}$$

From Equation (32), we can obtain $\dot{V}_2 < 0$ when $|\varepsilon_2| > \overline{F}_2/k_2$; thus,

$$|\varepsilon_2| \le \bar{\varepsilon}_2 \triangleq \max\left\{|\varepsilon_2(0)|, \frac{\overline{F}_2}{k_2}\right\}, \forall t \in \left[0, \tau_f\right) \tag{33}$$

When Equations (22) and (33) are combined, the range of conversion tracking errors can be concluded as follows.

$$-1 < T^{-1}(-\bar{\varepsilon}_2) \le \xi_2 \le T^{-1}(\bar{\varepsilon}_2) < 1, \forall t \in \left[0, \tau_f\right) \tag{34}$$

By Equations (21) and (34), it can be concluded that the control law a_2 is bounded. From Equations (7), (21), and (34), we can obtain $\left|\dot{a}_2\right| \le 2k_2\dot{\xi}_2/\left(1-\xi_2^{*2}\right)$, where $\xi_2^* = max\left\{T^{-1}(-\bar{\varepsilon}_2), T^{-1}(\bar{\varepsilon}_2)\right\}$. Hence, $\left|\dot{a}_2\right|$ is bounded for $t \in \left[0, \tau_f\right)$. The control laws are bounded for $t \in \left[0, \tau_f\right)$ according to Equation (21); thus, $\theta_1\int_{t-\tau_1}^{t} u(s)s$, $\theta_2\int_{t-\tau_2}^{t} x_2(s)s$, and $\theta_3\int_{t-\tau_3}^{t} x_3(s)s$ are bounded for $t \in \left[0, \tau_f\right)$.

Step 3: The Lyapunov function constructed for the third-order system is as follows:

$$V_3 = \frac{1}{2}\varepsilon_3^2 \tag{35}$$

By substituting Equations (12), (13), and (18) into the differential of Equation (35), we can obtain

$$\dot{V}_3 = \frac{2\varepsilon_3}{\left(1-\xi_3^2\right)\rho_3}\left[2\theta_2 z_2 + 2\theta_3\left(z_3 - \theta_1\int_{t-\tau_1}^{t} u(s)ds - \theta_2\int_{t-\tau_2}^{t} x_2(s)ds - \theta_3\int_{t-\tau_3}^{t} x_3(s)ds\right) - \dot{a}_2 - \xi_3\dot{\rho}_3 - \theta_1 k_3\varepsilon_3\right] \tag{36}$$

In Equation (36), $\xi_3 \in \Omega_{\tilde{\xi}}$ for $t \in \left[0, \tau_f\right)$ can be obtained from the above discussion, and based on the definition of ρ_3, we can obtain $\rho_3 > 0$ for $t \in [0, +\infty)$. Then, it can be concluded that $2/\left(\left(1-\xi_3^2\right)\rho_3\right) > 0$ for $t \in \left[0, \tau_f\right)$. $\dot{\rho}_3, \dot{a}_2$ are set as bounded. Define $F_3 = \left|2\theta_2 z_2 + 2\theta_3\left(z_3 - \theta_1\int_{t-\tau_1}^{t} u(s)ds - \theta_2\int_{t-\tau_2}^{t} x_2(s)ds - \theta_3\int_{t-\tau_3}^{t} x_3(s)s\right)\right| + |\dot{a}_2| + \left|\xi_3\dot{\rho}_3\right|$ and there exists a positive constant $\overline{F}_3$, such that $F_3 \le \overline{F}_3$ for $t \in \left[0, \tau_f\right)$. Then, $\dot{V}_3$ satisfies the following inequality.

$$\dot{V}_3 \le \frac{2|\varepsilon_3|}{\left(1-\xi_3^2\right)\rho_3}\left(\overline{F}_3 - \theta_1 k_3|\varepsilon_3|\right), \forall t \in \left[0, \tau_f\right) \tag{37}$$

From Equation (37), we can obtain $\dot{V}_3 < 0$ when $|\varepsilon_3| > \overline{F}_3/k_3$; thus,

$$|\varepsilon_3| \le \bar{\varepsilon}_3 \triangleq \max\left\{|\varepsilon_3(0)|, \frac{\overline{F}_3}{\theta_1 k_3}\right\}, \forall t \in \left[0, \tau_f\right) \tag{38}$$

Combining Equations (22) and (38), the range of conversion tracking errors can be concluded as follows.

$$-1 < T^{-1}(-\bar{\varepsilon}_3) \le \xi_3 \le T^{-1}(\bar{\varepsilon}_3) < 1, \forall t \in \left[0, \tau_f\right) \tag{39}$$

By Equations (21) and (39), it can be concluded that the control law u is bounded. From Equations (7), (21), and (39), we can obtain $|\dot{u}| \le 2k_3\dot{\xi}_3 / \left(1 - \xi_3^{*2}\right)$, where $\xi_3^* = max\{T^{-1}(-\bar{\varepsilon}_3), T^{-1}(\bar{\varepsilon}_3)\}$. Hence, $|\dot{u}|$ is bounded for $t \in \left[0, \tau_f\right)$. Owing to Equation (21), the control laws are bounded for $t \in \left[0, \tau_f\right)$; thus, $\theta_1 \int_{t-\tau_1}^{t} u(s)s$, $\theta_2 \int_{t-\tau_2}^{t} x_2(s)s$, and $\theta_3 \int_{t-\tau_3}^{t} x_3(s)s$ are bounded for $t \in \left[0, \tau_f\right)$.

According to Equations (29), (34), and (39), we can obtain that the normalized errors ξ, to satisfy $\xi \in \Omega_{\xi}$. Therefore, it can be concluded as follows with τ_f extending to $+\infty$.

$$\begin{aligned} -\rho_1 < z_1 - x_d < \rho_1 \\ -\rho_2 < z_2 - a_1 < \rho_2 \\ -\rho_3 < z_3 - a_2 < \rho_3 \end{aligned} \tag{40}$$

By performing inverse transformation based on Equation (18), it can be concluded for $t \in [0, +\infty)$ that

$$\begin{aligned} -\rho_1 < x_1 - x_d < \rho_1 \\ -\rho_2 < x_2 - a_1 < \rho_2 \\ -\rho_3 - \theta \int_{t-\tau}^{t} u(s)ds < x_3 - a_2 < \rho_3 - \theta \int_{t-\tau}^{t} u(s)ds \end{aligned} \tag{41}$$

where $\theta \int_{t-\tau}^{t} u(s)s = \theta_1 \int_{t-\tau_1}^{t} u(s)s + \theta_2 \int_{t-\tau_2}^{t} x_2(s)s + \theta_3 \int_{t-\tau_3}^{t} x_3(s)s$.

In summary, when the proposed control laws (9), (11), and (13) are applied to the electro-hydraulic servo pump-controlled system, the tracking error of the system can achieve prescribed performance convergence, and the proof for this conclusion is completed.

5. Experimental Results

In this section, the proposed PPC method accounting for input and state delays is programmed into the motion controller for experimental validation. This study conducts comparative experiments with the proposed method: a conventional PID controller and a traditional backstepping controller, which ignores time delays and aims to verify the effectiveness of the proposed algorithm. The introduction of the experimental platform and the presentation of experimental results are provided below.

5.1. Experimental Platform

As shown in Figure 2, the electro-hydraulic servo pump-controlled experimental platform consists of three core parts: the electrical drive system, the hydraulic drive system, and the actuator components.

The electrical drive system is composed of five key components: circuit breakers, a 24 V power supply, a motor controller, a motion controller, and relays. In the electrical drive system, circuit breakers serve to protect the circuit against overload and short-circuit damage, while the 24 V power supply supplies power to the system's controllers, sensors, and other low-voltage components to ensure the normal operation of low-power devices. The motor controller regulates the speed and torque of the servo motor based on command signals, enabling precise control of the motor's operating state; the motion controller is responsible for signal acquisition, algorithm computation, and control command generation. The hydraulic drive system is composed of five key components: a servo motor, a hydraulic

pump, accumulators, pressure sensors, and a hydraulic valve block. Among them, the servo motor serves as the system's core power source, while the hydraulic pump converts the motor's rotational speed and torque into the output pressure and flow of the hydraulic system. Meanwhile, accumulators are designed to store hydraulic oil and supplement the system's oil supply when needed, helping to stabilize the system's pressure and avoid oil shortage. Additionally, pressure sensors are responsible for collecting real-time pressure signals from the two chambers of the hydraulic cylinder. Finally, the hydraulic valve block integrates functional components of the system, such as check valves and relief valves, which not only simplifies the system's piping layout but also ensures the safe and reliable operation of the hydraulic circuits. The actuator component is composed of a displacement sensor, a hydraulic cylinder, and a load. Among these components, the hydraulic cylinder acts as the core executive element, driving the load to achieve linear displacement control. Meanwhile, the displacement sensor feeds back real-time displacement signals from the hydraulic cylinder to the motion controller, which provides critical data support to realize the system's closed-loop displacement control. The key parameters of the experimental platform are presented in Table 1.

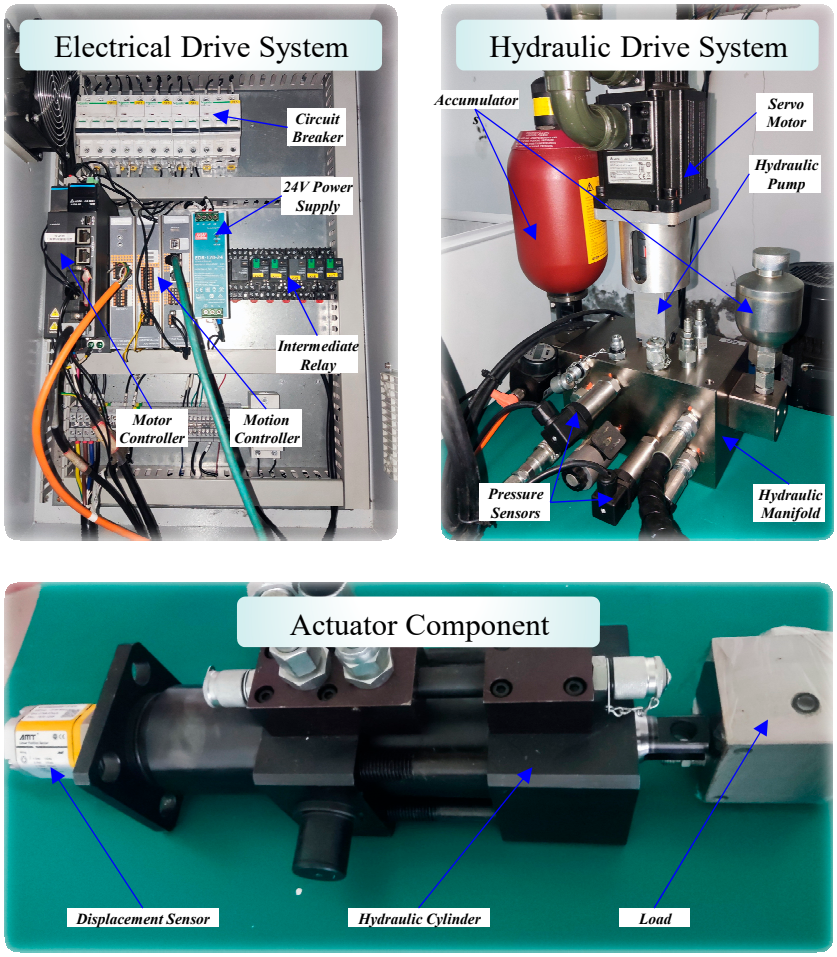


Figure 2. The experimental platform for electro-hydraulic servo pump-controlled systems.

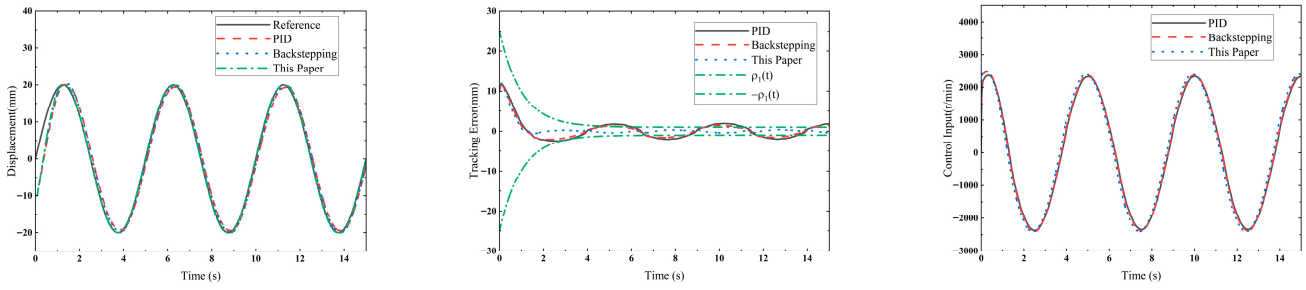
Table 1. Key component parameters of the experimental platform.

Component Name	Parameter Name	Parameter Value
Servo Motor	Rated Voltage Rated Speed Rated Power	220 V AC 3000 r/min 1 KW
Hydraulic Pump	Rated Working Pressure Displacement Maximum Speed Minimum Speed	21 MPa 0.8 cc 3000 r/min 500 r/min
Accumulator	Volume Inflation Pressure	1 L 0.6 bar
Pressure Sensors	Measurement Range	0–40 MPa
Displacement Sensor	Type Measurement Range Resolution	Magnetostriction 60 mm 0.001 mm
Hydraulic Cylinder	Stroke Bore Rod Diameter Displacement Accuracy	60 mm 50 mm 30 mm 0.01 mm

5.2. Experimental Analysis

The time-delay parameters are measured as $\tau_1 = 10$ ms, $\tau_2 = 15$ ms, and $\tau_3 = 15$ ms. The system parameters are selected as $\theta_1 = 2.17 \times 10^7$, $\theta_2 = 6.08 \times 10^7$, and $\theta_3 = 1.28 \times 10^8$. The PID parameters are tuned based on the Ziegler–Nichols method and are selected as $P = 195$, $I = 3.5$, and $D = 0.1$. The parameters of the backstepping controller are $c_1 = 4 \times 10^6$, $c_2 = 9.3 \times 10^5$, and $c_3 = 12$. The parameters of the proposed control method are set as $k_1 = 32$, $k_2 = 6$, and $k_3 = 12.8$. The values of state variables $x_1(t)$, $x_2(t)$, and $x_3(t)$ are provided by the displacement sensor and pressure sensors.

In the first experiment, a sine signal with an amplitude of 20 mm and a frequency of 0.2 HZ is adopted as the reference signal. In the PPC method proposed in this paper, the initial value of the performance function is set as $\rho_1^0 = 25$, the steady-state error value is $\rho_1^0 = 25$ and the attenuation rate is $\lambda_1 = 1$. The initial displacement of the hydraulic cylinder is –10 mm. The experimental results are shown in Figure 3.



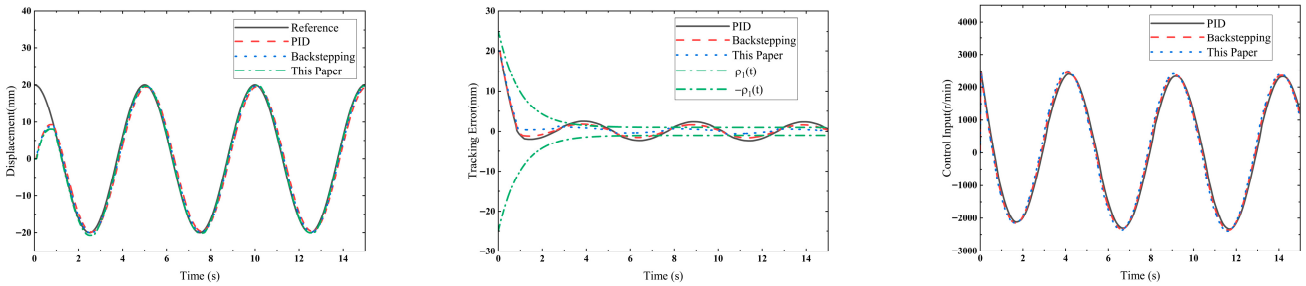
(**a**) Trajectory tracking. (**b**) Tracking error. (**c**) Control input.

Figure 3. Experimental results for sine reference signal.

The trajectory tracking curves of the hydraulic cylinder are shown in Figure 3a. The PPC method proposed in this paper achieves the command sine signal at 1.06 s, and then the displacement curve almost completely overlaps the reference curve. Compared to the PID controller and the backstepping controller, the prescribed performance controller has the best response speed and control accuracy. The trajectory tracking errors of the three

methods are shown in Figure 3b. The trajectory tracking error of the PPC method converges quickly and is always constrained within the performance boundary, while the trajectory tracking errors of the PID controller and backstepping controller cannot be guaranteed to be within a stable range. The control input signal is shown in Figure 3c, with the maximum motor speed being 2500 r/min.

In the second experiment, a cosine signal with an amplitude of 20 mm and a frequency of 0.2 HZ is adopted as the reference signal. In the PPC method proposed in this paper, the initial value of the performance function is set as $\rho_1^0 = 25$, the steady-state error value is $\rho_1^0 = 25$, and the attenuation rate is $\lambda_1 = 1$. The initial displacement of the hydraulic cylinder is 0 mm. The experimental results are shown in Figure 4.



(**a**) Tracking trajectory. (**b**) Tracking error. (**c**) Control input.

Figure 4. Experimental results for cosine reference signal.

The trajectory tracking curves of the hydraulic cylinder are shown in Figure 4a. The PPC method proposed in this paper achieves a command cosine signal at 0.90 s, and then the displacement curve almost completely overlaps with the reference curve. Compared to the PID controller and the backstepping controller, the prescribed performance controller has the best response speed and control accuracy. The trajectory tracking errors of the three methods are shown in Figure 4b. The trajectory tracking error of the PPC method converges quickly and is always constrained within the performance boundary, while the trajectory tracking errors of the PID and backstepping controllers are not guaranteed to remain within a predefined range. The control input signal is shown in Figure 4c.

There are two distinctions between the first and second experiments. The first difference is the initial tracking error. The initial tracking error is set to 10 mm in the first experiment and 20 mm in the second. The purpose of this design is to verify whether the system can converge according to the prescribed performance under different initial tracking errors, thus verifying the transient performance of the proposed method under varying initial conditions. The second difference is the phase of the reference signals. The purpose of this design is to verify the robustness of the proposed method to different phase reference signals. The use of cosine signals with the same frequency in the second experiment is not a mere repetition; instead, it is a targeted design intended to verify the system's robustness to signal phase changes.

In conclusion, compared to PID and backstepping controllers, the PPC method proposed in this paper exhibits the advantages of fast response, high-precision tracking, strong error constraint, and stable control input. The combination of PPC and the Lyapunov–Krasovskii method can effectively improve the control accuracy and dynamic response of the system with time delays.

6. Conclusions

Focusing on the time-delay phenomena in the position control of electro-hydraulic servo pump-controlled systems, this paper establishes the state-space representation of

the electro-hydraulic servo pump-controlled system by incorporating input delays and state delays and innovatively integrates the Lyapunov–Krasovskii method with PPC to achieve the system's prescribed performance position control. Experimental results show that the proposed method can constrain the convergence speed and steady-state accuracy of trajectory tracking errors within the performance boundaries, which is superior to the traditional PID and backstepping control methods. The research results of this paper can be extended to fields such as robotic motion control and precision manufacturing, which offer significant value in improving the motion accuracy, operational stability, and production efficiency of equipment.

Author Contributions: Conceptualization, G.Q. and Y.H.; methodology, G.Q.; software, Y.H.; validation, G.Q., Y.H. and G.C.; formal analysis, G.Q.; investigation, G.Y.; resources, Y.C.; data curation, Y.H.; writing—original draft preparation, G.Q.; writing—review and editing, G.Q.; visualization, G.Q.; supervision, G.C.; project administration, G.Y.; funding acquisition, G.C. All authors have read and agreed to the published version of the manuscript.

Funding: This research was funded by the National Natural Science Foundation of China, grant number 52275066; 'Tianchi Talent' Introduction Programme, grant number 2024XGYTCYC02; the Major Science and Technology Projects of the 12th Division Science and Technology Bureau of Xinjiang Production and Construction Corps in 2022, grant number SRS2022003; the Natural Science Foundation of Xinjiang Uygur Autonomous Region, grant number 2025D01E18; and the National Key Laboratory of Metal Forming Technology and Heavy Equipment, grant number SKLMF-2025-025.

Data Availability Statement: The original contributions presented in the study are included in the article, further inquiries can be directed to the corresponding author.

Conflicts of Interest: The author Yao Chen was employed by the Shougang Jingtang United Iron & Steel Co., Ltd. The remaining authors declare that the research was conducted in the absence of any commercial or financial relationships that could be construed as a potential conflict of interest.

References

1. Liu, H.; Zhang, X.; Quan, L.; Zhang, H. Research on energy consumption of injection molding machine driven by five different types of electro-hydraulic power units. *J. Clean. Prod.* **2020**, *242*, 118355. [CrossRef]
2. Qin, S.; Zhang, H.; Jiang, H.; Xu, W.; Qu, J. Amplitude–frequency characteristics during the volume-pulsatile packing process. *J. Manuf. Sci. Eng.* **2021**, *143*, 111007. [CrossRef]
3. Xu, Z.; Liu, Y.; Hua, L.; Zhao, X.; Wang, X. Energy improvement of fineblanking press by valve-pump combined controlled hydraulic system with multiple accumulators. *J. Clean. Prod.* **2020**, *257*, 120505. [CrossRef]
4. Xu, J.; Du, H.; Zhou, S.; Wei, L.; Chen, P.; Zheng, Y. Energy-efficient design and power flow analysis of electro-hydraulic steering systems for heavy-duty wheeled vehicles via parameter identification. *Energy* **2025**, *322*, 135562. [CrossRef]
5. Quan, Z.; Ge, L.; Wei, Z.; Li, Y.; Quan, L. A survey of powertrain technologies for energy-efficient heavy-duty machinery. *Proc. IEEE* **2021**, *109*, 279–308. [CrossRef]
6. Jiao, Z.; Li, Z.; Shang, Y.; Wu, S.; Song, Z.; Pan, Q. Active load sensitive electro-hydrostatic actuator on more electric aircraft: Concept, design, and control. *IEEE Trans. Ind. Electron.* **2021**, *69*, 5030–5040. [CrossRef]
7. Ding, R.; Mu, X.; Cheng, M.; Xu, B.; Li, G. Terminal force soft sensing of hydraulic manipulator based on the parameter identification. *Measurement* **2022**, *200*, 111551. [CrossRef]
8. Ba, K.; Wang, Y.; He, X.; Wang, C.; Yu, B.; Liu, Y.; Kong, X. Force compensation control for electro-hydraulic servo system with pump–valve compound drive via QFT–DTOC. *Chin. J. Mech. Eng.* **2024**, *37*, 27. [CrossRef]
9. Yan, G.; Zhang, T.; Liu, X.; Yao, C.; Ai, C. The ADRC strategy research of electro-hydraulic servo pump control system based on dynamic load torque compensation for high-performance force control. *Int. J. Electr. Power Energy Syst.* **2025**, *171*, 110991. [CrossRef]
10. Shi, S.; He, Z.; Zeng, D.; Huang, P.; Jin, G. Identification and Modeling of a Servo Pump-Controlled Hydraulic System. *IEEE/ASME Trans. Mechatron.* **2024**, *30*, 2551–2561. [CrossRef]
11. Liu, J.; Xia, Y.; Liu, G.; Lyu, L.; Nie, Y.; Mei, D. Motion Control of Electro-Hydrostatic Actuators with Modeling and Compensation of Nonlinear Bulk Modulus. *IEEE Trans. Ind. Electron.* **2024**, *72*, 6185–6193. [CrossRef]

12. Li, S.; Zhang, Z.; Ding, K.; Guo, K.; Zhao, J.; Du, H. High-dynamic steering control of the pump-controlled electro-hydraulic steering system for heavy vehicles with active disturbance suppression. *J. Franklin Inst.* **2024**, *361*, 107107. [CrossRef]
13. Léchappé, V.; Rouquet, S.; Gonzalez, A.; Plestan, F.; León, J.; Moulay, E. Delay estimation and predictive control of uncertain systems with input delay: Application to a DC motor. *IEEE Trans. Ind. Electron.* **2016**, *63*, 5849–5857. [CrossRef]
14. Liang, W.; Sun, P.; Zhao, W.; Wang, C.; Luan, Z.; Liu, L. Variable Gain Robust Pressure Tracking Control for Integrated Brake-By-Wire System under Time-Varying Hydraulic Time Delay. *IEEE Trans. Transp. Electrif.* **2025**, *11*, 8797–8810. [CrossRef]
15. Helian, B.; Chen, Z.; Yao, B.; Lyu, L.; Li, C. Accurate motion control of a direct-drive hydraulic system with an adaptive nonlinear pump compensation. *IEEE/ASME Trans. Mechatron.* **2020**, *26*, 2593–2603. [CrossRef]
16. Yao, Z.; Yao, J. Exponential Asymptotic Prescribed Performance Control of Electro-Hydrostatic Actuators. *IEEE Trans. Ind. Electron.* **2025**, *72*, 9675–9685. [CrossRef]
17. Yang, R.; Liu, G.P.; Shi, P.; Thomas, C.; Basin, M.V. Predictive output feedback control for networked control systems. *IEEE Trans. Ind. Electron.* **2013**, *61*, 512–520. [CrossRef]
18. Coskun, M.Y.; Itik, M. Intelligent PID control of an industrial electro-hydraulic system. *ISA Trans.* **2023**, *139*, 484–498. [CrossRef]
19. Zhang, Z.; Chen, S.; Zheng, Y. Fully distributed scaled consensus tracking of high-order multiagent systems with time delays and disturbances. *IEEE Trans. Ind. Inform.* **2021**, *18*, 305–314. [CrossRef]
20. Cai, Y.; Ren, G.; Song, J.; Sepehri, N. High precision position control of electro-hydrostatic actuators in the presence of parametric uncertainties and uncertain nonlinearities. *Mechatronics* **2020**, *68*, 102363. [CrossRef]
21. Truong, H.V.A.; Nam, S.; Kim, S.; Kim, Y.; Chung, W. Backstepping-sliding-mode-based neural network control for electro-hydraulic actuator subject to completely unknown system dynamics. *IEEE Trans. Autom. Sci. Eng.* **2023**, *21*, 6202–6216. [CrossRef]
22. Wang, M.; Wang, Y.; Yang, R.; Fu, Y.; Zhu, D. A Sliding Mode Control Strategy for an ElectroHydrostatic Actuator with Damping Variable Sliding Surface. *Actuators* **2021**, *10*, 3. [CrossRef]
23. Ahn, K.K.; Nam, D.N.C.; Jin, M. Adaptive backstepping control of an electrohydraulic actuator. *IEEE/ASME Trans. Mechatron.* **2013**, *19*, 987–995. [CrossRef]
24. Ren, G.; Costa, G.K.; Sepehri, N. Position control of an electro-hydrostatic asymmetric actuator operating in all quadrants. *Mechatronics* **2020**, *67*, 102344. [CrossRef]
25. Liu, Y.; Gao, J.; Luo, Y.; Zhang, L. Robust smith predictor-based internal model nonlinear control with lead compensation extended state observer for pmlsm servo systems considering time delay. *IEEE Trans. Power Electron.* **2024**, *39*, 5424–5438. [CrossRef]
26. Furtat, I.; Fridman, E.; Fradkov, A. Disturbance compensation with finite spectrum assignment for plants with input delay. *IEEE Trans. Autom. Control* **2017**, *63*, 298–305. [CrossRef]
27. Lu, Y.; Liu, W.; Ma, B. Finite-time command filtered tracking control for time-varying full state-constrained nonlinear systems with unknown input delay. *IEEE Trans. Circuits Syst. II Express Briefs* **2022**, *69*, 4954–4958. [CrossRef]
28. Li, D.; Liu, Y.; Tong, S.; Chen, C.L.P.; Li, D. Neural networks-based adaptive control for nonlinear state constrained systems with input delay. *IEEE Trans. Cybern.* **2018**, *49*, 1249–1258. [CrossRef]
29. Li, Z.; Chen, H.; Lam, H.K.; Wu, W.; Zhang, W. Switched command-filtered-based adaptive fuzzy output-feedback funnel control for switched nonlinear MIMO-delayed systems. *IEEE Trans. Fuzzy Syst.* **2024**, *32*, 6560–6572. [CrossRef]
30. Bechlioulis, C.P.; Rovithakis, G.A. Robust adaptive control of feedback linearizable MIMO nonlinear systems with prescribed performance. *IEEE Trans. Autom. Control* **2008**, *53*, 2090–2099. [CrossRef]
31. Xu, X.; Hou, M.; Duan, G. Dynamic Periodic Event-Triggered Adaptive Prescribed Performance Control of Uncertain Semi-Strict Feedback Systems with Application. *IEEE Trans. Circuits Syst. I Regul. Pap.* **2025**, *72*, 4248–4260. [CrossRef]
32. Zhang, C.; Guo, G.; Liu, Y.; Yang, G. Low-complexity prescribed performance control of nonlinear systems with full-state constraints. *IEEE Trans. Circuits Syst. II Express Briefs* **2023**, *71*, 2254–2258. [CrossRef]
33. Sui, S.; Chen, C.L.P.; Tong, S. Finite-time adaptive fuzzy prescribed performance control for high-order stochastic nonlinear systems. *IEEE Trans. Fuzzy Syst.* **2021**, *30*, 2227–2240. [CrossRef]
34. Chen, G.; Dong, J. Approximate optimal adaptive prescribed performance control for uncertain nonlinear systems with feature information. *IEEE Trans. Syst. Man Cybern. Syst.* **2024**, *54*, 2298–2308. [CrossRef]
35. Sheng, Z.; Ma, Q.; Xu, S. Sampled-data practical tracking control for nonlinear time-delay systems. *IEEE Trans. Circuits Syst. II Express Briefs* **2021**, *69*, 1272–1276. [CrossRef]
36. Yuan, M. Dynamic event-triggered output feedback control for a class of high-order feedforward nonlinear time-delay systems. *IEEE Trans. Circuits Syst. II Express Briefs* **2021**, *68*, 3436–3440. [CrossRef]

Disclaimer/Publisher's Note: The statements, opinions and data contained in all publications are solely those of the individual author(s) and contributor(s) and not of MDPI and/or the editor(s). MDPI and/or the editor(s) disclaim responsibility for any injury to people or property resulting from any ideas, methods, instructions or products referred to in the content.